Acta Tropica 247 (2023) 107005

Contents lists available at ScienceDirect

Acta Tropica

journal homepage: www.elsevier.com/locate/actatropica

Evolving immunometabolic response to the early *Leishmania infantum* infection in the spleen of BALB/c mice described by gene expression profiling

Génesis Palacios [a], Raquel Diaz-Solano [a], Basilio Valladares [a,b], Roberto Dorta-Guerra [a,c], Emma Carmelo [a,b,*]

[a] Instituto Universitario de Enfermedades Tropicales y Salud Pública de Canarias (IUETSPC), Universidad de La Laguna (ULL), Avenida Astrofísico Francisco Sánchez s/n (Tenerife), La Laguna 38200, Spain
[b] Departamento de Obstetricia y Ginecología, Pediatría, Medicina Preventiva y Salud Pública, Toxicología, Medicina Legal y Forense y Parasitología, Universidad de La Laguna, (Tenerife), La Laguna 38200, Spain
[c] Departamento de Matemáticas, Estadística e Investigación Operativa, Facultad de Ciencias, Universidad de La Laguna, (Tenerife), La Laguna 38200, Spain

ARTICLE INFO

Keywords:
Transcriptional changes
Gene expression profile
Over-represented pathways
Leishmania infantum
Mice spleen
Visceral leishmaniasis

ABSTRACT

Transcriptional analysis is a useful approximation towards the identification of global changes in host-pathogen interaction, in order to elucidate tissue-specific immune responses that drive the immunopathology of the disease. For this purpose, expression of 223 genes involved in innate and adaptive immune response, lipid metabolism, prostaglandin synthesis, C-type lectin receptors and MAPK signaling pathway, among other processes, were analyzed during the early infection in spleens of BALB/c mice infected by *Leishmania infantum*. Our results highlight the activation of immune responses in spleen tissue as early as 1 day p.i., but a mixed pro-inflammatory and regulatory response at day 10 p.i., failing to induce an effective response towards control of *Leishmania* infection in the spleen. This ineffective response is coupled to downregulation of metabolic markers relevant for pathways related to icosanoid biosynthesis, adipocytokine signaling or HIF-1 signaling, among others. Interestingly, the over-representation of processes related to immune response, revealed *Il21* as a potential early biomarker of *L. infantum* infection in the spleen. These results provide insights into the relationships between immune and metabolic responses at transcriptional level during the first days of infection in the *L. infantum*-BALB/c experimental model, revealing the deregulation of many important pathways and processes crucial for parasitic control in infected tissues.

1. Introduction

Visceral leishmaniasis (VL) is an infectious disease caused by parasites of the *Leishmania* genus, which is transmitted through the bite of infected sandflies. VL is caused by *L. donovani* or *L. infantum* (Kaye and Scott, 2011), affecting mainly spleen, liver and bone marrow. VL is characterized by a wide range of symptoms including prolonged fever, weight loss, anemia, splenomegaly, hepatomegaly and immunosuppression, and can be fatal if untreated. It is estimated that there are 50,000 to 90,000 new cases of VL worldwide every year, with the majority of cases occurring in India, Bangladesh, Sudan, Ethiopia, and Brazil (Singh et al., 2006).

Murine model has been useful in the study of immune responses for the elimination vs. persistence of the parasite during VL. In mice, the immune response is compartmentalized, with the granulomatous response leading to clearance of parasites in the liver, while the persistence of parasites in the spleen results in a lifelong chronic infection, particularly when high infective inoculums are used (Oliveira et al., 2012; Poulaki et al., 2021; Rodrigues et al., 2016; Rolão et al., 2004). The outcome of the experimental infection depends on several factors, such as the host immunity, the strain virulence, the number of inoculated parasites and the route of inoculation (Melby et al., 1998; Rolão et al., 2004; Titus and Ribeiro, 1988). The spleen structure is divided in rodents in the red and white pulp, and between these two regions is the

* Corresponding author at: Instituto Universitario de Enfermedades Tropicales y Salud Pública de Canarias (IUETSPC), Universidad de La Laguna (ULL), Avenida Astrofísico Francisco Sánchez s/n (Tenerife), La Laguna 38200, Spain.
E-mail address: ecarmelo@ull.edu.es (E. Carmelo).

https://doi.org/10.1016/j.actatropica.2023.107005
Received 25 May 2023; Received in revised form 27 July 2023; Accepted 21 August 2023
Available online 22 August 2023

marginal zone (MZ) (Lewis et al., 2019). Marginal zone macrophages (MZM), marginal metallophilic macrophages (MMM), and red pulp macrophages are the splenic populations that phagocytize >95% of L. *donovani* amastigotes (Gorak et al., 1998).

In the initial contact with the parasite, marginal zone macrophages (MZM) present parasitic promastigote antigens (Kaye et al., 2004; Tibúrcio et al., 2019). Protective responses in the spleen are generated by dendritic cells (DCs) exposed to parasite products, but not productively infected by *Leishmania* (bystander DCs) (Rodrigues et al., 2016). The differentiation of Th1 or Th17 cells is mounted by cytokines produced by bystander DCs, and these cells also prime naïve CD8 T cells. In contrast, in infected DCs, the parasite seizes the capacity of the cell to initiate protective responses. The combined secretion of cytokines such as IL-12, IL-27 and IL-10 by infected DCs leads to the differentiation of Tr1 cells that simultaneously produce IFN-γ and IL-10 and decrease the leishmanicidal capacity of the macrophage. Additionally, exhaustion of specific CD8 T cells is promoted by upregulating the expression of inhibitory receptors such as PD-1 or LAG-3 (Rodrigues et al., 2016).

In the chronic phase of VL, infection leads to splenomegaly and the mouse spleen suffers dramatic changes in microarchitecture, including disorganization of the white pulp, hypertrophy of the red pulp and disruption of the marginal zone (Kaye et al., 2004; Melo et al., 2020; Rodrigues et al., 2016). *L. donovani* infection in mice spleen generates loss of red pulp/white pulp differentiation and the onset of extramedullary hematopoiesis (Ashwin et al., 2019). The chronicity of the infection in the spleen is due to the release of inhibitory substances, such as IL-10 and TGF-β, by myeloid suppressor cells (MDSC) (Abidin et al., 2017; Osorio et al., 2020). Moreover, the hypoxic environment of the spleen increases the stability of hypoxia-inducible factor 1 (HIF1), which reduces the ability of dendritic cells (DC) to produce IL-12 and promotes the release of IL-10 (Hammami et al., 2018, 2017).

The Syrian golden hamster is the most suitable experimental model for studying VL, as it accurately replicates the pathophysiological characteristics observed in humans. However, the limited availability of reagents for immunological and molecular studies has led to the extensive use of murine model for experimental purposes; this also renders results that are easier to compare to most of the available literature (Loria-Cervera and Andrade-Narvaez, 2014; Saini and Rai, 2020). In the study of disease progression, the transcriptional analysis has been an useful approximation towards the identification of global changes at tissue level in the host-pathogen interaction, in order to elucidate tissue-specific immune responses that lead towards the immunopathology in VL (Ashwin et al., 2019; Engwerda and Kaye, 2000; Forrester et al., 2022; Negron et al., 2004; Palacios et al., 2021). Recent studies have also looked into the relationship between immune and metabolic responses at transcriptional level, either in bone-marrow-derived macrophages or in the initial invasion of the spleen, up to 24 h post-infection (Palacios et al., 2023; Rabhi et al., 2012). In this paper, the transcriptional changes in the early infection of the spleen were analyzed, in order to obtain insights of the most important differentially expressed genes over time. For this purpose, expression of 223 genes involved in innate and adaptive immune response, lipid metabolism, prostaglandin synthesis, C-type lectin receptors and MAPK signaling pathway, among other processes, were analyzed at 1-, 3-, 5- and 10- days p.i. (post infection) in spleens of mice infected by *L. infantum*.

Our results highlight the activation of immune responses in spleen tissue as early as 1 day p.i., but a mixed pro-inflammatory and regulatory response at day 10 p.i., failing to induce an effective response towards control of *Leishmania* infection in the spleen. This ineffective response is coupled to downregulation of metabolic markers relevant for pathways related to icosanoid biosynthesis, adipocytokine signaling or HIF-1 signaling, among others. Interestingly, the over-representation of processes related to immune response, revealed *Il21* as a potential early biomarker of *L. infantum* infection in the spleen.

2. Materials and methods

2.1. Biological samples

This study utilized forty-eight female wild-type BALB/c mice (7 weeks old) provided by Charles River Laboratories, France. Animals were maintained in a specific pathogen-free environment at ULL. To conduct the experiment, the animals were randomly divided into two groups: 24 control mice and 24 mice that were inoculated with 100 μl of PBS with 10^6 promastigotes of *L. infantum* (JPC strain, MCAN/ES/98/LLM-724) in stationary growth phase via the coccygeal vein on day 0 of the experiment. *L. infantum* was maintained *in vivo* through serial murine passages. Prior to infection, amastigote-derived promastigotes were amplified by culture in RPMI medium (Gibco BRL, Grand Island, NY, USA) containing 20% inactivated fetal calf serum (SBFI), 100 ug/ml streptomycin (Sigma-Aldrich, St. Louis, USA), and 100 U/ml of penicillin (Biochrom AG, Berlin, Germany) at 26 °C until reaching stationary phase with less than 3 passages *in vitro*.

The spleens of 6 infected and 6 control mice ($n = 12$ for each time point) were extracted after cervical dislocation at 1, 3, 5, and 10 days post-infection (days p.i.). Spleen weight was determined and a fragment (10–40 mg) of the thinner end of the spleen was taken to determine parasitic load by quantitative limiting-dilution (Buffet et al., 1995). The rest of the spleen was divided in 7–10 mg aliquots and immediately stored in RNA later at −80 °C (Sigma-Aldrich, St. Louis, USA) for nucleic acid preservation and later mRNA extraction.

2.2. RNA isolation and quantification

Preserved spleen tissue (7–10 mg) was used for RNA isolation in Lysing Matrix D columns (MP Biomedicals, Solon, USA) and using FastPrep®System (ProSci- entific, Cedex, France); RNA quantification was performed as previously described (Palacios et al., 2021). DeNovix DS-11 Spectrophotometer (DeNovix) was used to quantify and evaluate RNA purity. Only samples with OD260/280 ratios between 1.96–2.14 and ratio OD260/230 between 1.79- 2.29 were included in this study. The RNA integrity was evaluated with RNA 6000 Nano Kit chips (Agilent Technologies, Santa Clara, USA) on a 2100 Bioanalyzer (Agilent Technologies, Santa Clara, USA). All RNA samples used in the study had a RNA integrity number (RIN) >7, indicating high quality. Furthermore, agarose gel electrophoresis was conducted on all RNA samples to ensure their integrity and quality.

2.3. Reverse transcription and high-throughput real-time quantitative PCR (RT-qPCR)

Reverse transcription and Real Time qPCR was performed, using High-Capacity cDNA Reverse Transcription kit (Thermo Fisher Scientific), as previously described (Gómez et al., 2021; Hernandez-Santana et al., 2016; Palacios et al., 2021). Real Time qPCR was carried out using OpenArray® plates with TaqMan probes (Thermo Fisher) for the amplification of 223 genes previously selected after an extensive literature review; all genes were related to immune and metabolic processes. Thermo Fisher Scientific commercially designed all primers and probes (Table S1). Each plate allowed performing 3072 amplification reactions. The plate was organized in 48 subarrays, each with 64 nanopockets. PCR mixture was prepared following the manufacturer's instructions and plates were loaded using the Accufill™ System (Thermo Fisher Scientific). Each amplification reaction was performed in a volume of 33 nl. The thermal cycle and fluorescence detection were performed with the QuantStudio™ 12 K Flex Real-Time PCR System (Thermo Fisher Scientific) following manufacturer's recommendations.

2.4. Data pre-processing and processing

MS Excel was used to import data from QuantStudio™ 12 K Flex

Real-Time PCR System software, and the arithmetic average quantitative cycle (Cq) was employed for the purpose of data analysis. Two mice (5R2NRB and 10R1RB) showed outlier *Cq* values compared to their biological group and for this reason, those mice were removed of subsequent gene expression analyses. *GenEx* (MultiD) software was used for data preprocessing and normalization. Before normalization, reference genes were selected in *GenEx* using two different methods: geNorm (setting M-value lower than 0.5) and NormFinder, revealing three genes that showed the most stable expression: *Hif1a, Erk2, Hprt*. Normalization with these genes was performed to obtain Normalized Relative Quantities (NRQ) values. For subsequent analyses, results for endogenous genes' expression were excluded.

2.5. Statistical analysis

For each measured parameter, the mean and its standard error (SEM) were calculated, and outliers were examined using boxplots and studentized residuals. Normality of the data distribution was evaluated using the Kolmogorov-Smirnov test or Shapiro-Wilk test, as appropriate, and the homogeneity of variance was assessed with the Levene test. The differences in parasite burden between timepoints were determined by a one-way Analysis of Variance (ANOVA). Tukey's test as post hoc comparison technique was carried out to compare the means from different groups. Difference in spleen weight between infected and control mice at each timepoint was determined by the subtraction of the spleen weight of each infected mice and the mean spleen weight of control mice at each timepoint; statistical differences in spleen weight between infected and control mice were analyzed by two tail unpaired *t*-test or two tail Mann-Whitney U test, as appropriate.

NRQ values were used for individual gene representation and representations of differential gene expression. Fold change of gene expression was calculated as the ratio between the average gene expression in the infected group and non-infected-control mice and expressed as Log_2. Statistical differences in NRQ values were analyzed by two tail unpaired *t*-test or two tail Mann-Whitney U test, as appropriate, using GraphPad Prism version 9.2.0, GraphPad Software, San Diego California USA (www.graphpad.com).

2.6. Representations of differential gene expression

Differentially expressed genes (DEGs) between infected and control mice at each timepoint were represented in STRING Interaction networks, volcano plots and heatmaps. The criteria to consider differentially expressed genes (DEGs) were the statistical significance threshold (p-value < 0.05) and the biological significance threshold $\log_2FC>1$ or $\log_2FC<-1$ (corresponding to FC > 2 and FC < 0.5 respectively).

In STRING Interaction Network, color nodes represent Log_2FC of gene expression; intensity of color nodes indicates upregulation (deeper red intensity) and downregulation (deeper blue intensity). For network representations, Prefuse Force directed layout was applied. Line thickness indicates the stringdb interaction score. The active interaction sources come from textmining, coexpression, databases and experiment. Minimum required interaction score is high confidence (0.8). These graphics were obtained in Cytoscape 3.8.2 (http://www.cytoscape.org).

In Volcano plots, genes passing biological significance threshold and statistical significance threshold were represented in red and blue, attending to their upregulation and downregulation, respectively. Volcano plots were made by plotting $-\log_{10} p$-value (determined by two tail Mann–Whitney U test) on the y-axis, and $\log_2$ of FC on the x-axis. These graphics were generated using SPSS version 26 (IBM Corporation, Armonk, NY, USA) statistical software.

Heatmaps showing the differential expression of genes in control and infected mice were obtained after unsupervised hierarchal clustering of the autoscaled NRQ values, based on Euclidean distance and pairwise average-linkage. These graphics were obtained in Cytoscape 3.8.0 (http://www.cytoscape.org/) (Shannon, 2003) using the plugin clusterMaker (Morris et al., 2011).

2.7. STRING functional enrichment analysis

With the list of DEGs between infected and control mice at each timepoint, functional enrichment analysis was performed in Cytoscape 3.8.2 (http://www.cytoscape.org). Enrichment analysis was performed either with upregulated and downregulated genes at each timepoint, using genes passing both biological significance threshold and statistical significance threshold as in volcano plots. Before STRING functional enrichment analysis, GO Process, KEGG Pathways and Reactome Pathways categories were selected and redundant terms were removed (redundancy cutoff: 0.25). Enriched pathways were ordered by FDR value (threshold FDR <0.05) this measure describes how significant the enrichment is; p-values corrected for multiple testing within each category using the Benjamini-Hochberg procedure (Szklarczyk et al., 2017). Top ten enriched pathways were selected to posterior interpretation. To compare enrichment results among timepoints, we also performed functional enrichment analysis without removing redundant terms (Table S2).

Over-represented pathways were obtained from enrichment analysis using only upregulated or downregulated DEGs at each timepoint

3. Results

3.1. Parasite burden and changes in spleen weight after L. infantum infection

One day after parasite inoculation, mean parasitic burden in spleen of infected mice was 6.7×10^3 parasites/g tissue, confirming the infection was stablished in the spleen. The parasitic load was relatively stable for the first 3 days p.i., but jumped on 5 days p.i.-mice ($p<0.01$) and 10 days p.i.-mice ($p<0.001$) (Fig. 1A). Results show that at 5 days p.i., there is a leap in the parasite burden in spleen, similarly to what was observed in the liver (Palacios et al., 2021).

Regarding spleen weight, the difference between infected and control mice is statistically significant as early as 1 day p.i (Fig. 1B). Our results show that the spleen weight is increasing steadily during the course of the experiment (Fig. 1B).

3.2. Gene expression changes over the early L. infantum infection in BALB/c mice

At 1 day p.i., 71 genes were differentially expressed, 67 of them upregulated with statistically significant differences (red dots in Fig. 2A and B) and 4 of them statistically downregulated (blue dots in Fig. 2A and C). Heatmap reveals two main clusters of genes that separate infected- and control- mice according to their gene expression (Fig. 2D).

This general upregulation of genes was reduced at 3 days p.i., with 31 genes differentially expressed, 19 of them were statistically significant upregulated (red dots in Fig. 3A and B) and 12 of them were statistically significant downregulated (blue dots in Fig. 3A and C). The connections among these DEGs are represented in a STRING interaction network (Fig. 3D) that shows a main cluster constituted by upregulated interleukin and CD-coding genes, except *Socs1,* that was significantly downregulated (Fig. 3B). The second cluster is composed by downregulated chemokine and chemokine receptors (*Ccl9, Cxcl1, Cxcl2, Cxcl10*) and also by *Ptgfr*. The third cluster was formed by inflammation related genes, all downregulated (*Alox5, Alox12, Ptges3)* with the exception of *Ptgs2*.

Contrary to previous observations, predominant downregulation of genes was observed at 5 days p.i, with 46 genes differentially expressed (DE) between infected and control mice, 9 of them were statistically significant upregulated (red dots in Fig. 4A and B) and 37 of them were statistically significant downregulated (blue dots in Fig. 4A and C).

Heatmap in Fig. 4D shows the separation of infected and control

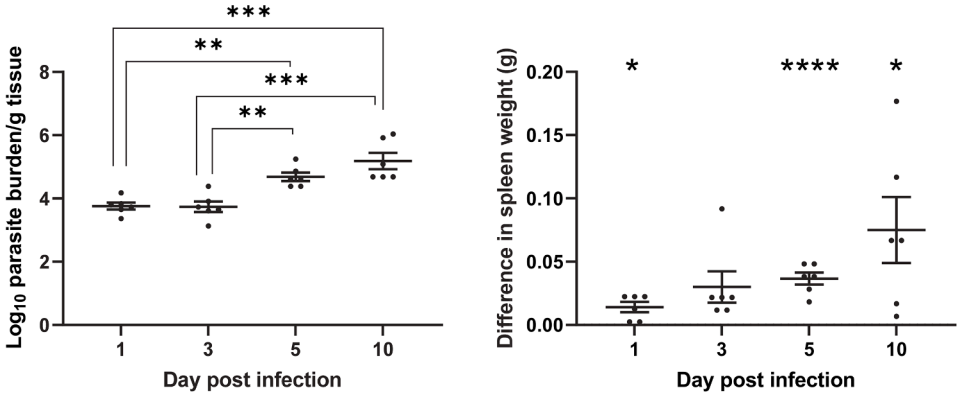

Fig. 1. (A) Evolution of parasite burden in spleen. Mice were inoculated with 1×10^6 promastigotes i.v. Parasite load was determined on 1 day ($n = 6$), 3 days ($n = 6$), 5 days ($n = 6$) and 10 days ($n = 6$) p.i. by limiting dilution assay and expressed as $\log_{10}$ of the average parasite load per gram of tissue. Error bars indicate SEM. (B) Difference in spleen weight of each infected animal ($n = 6$) and the mean of spleen weight of control mice at each timepoint. (Spleen weight of each infected mice – Mean spleen weight of control mice). Error bars indicates SEM. Statistically significant differences are indicated (*$p < 0.05$, **$p < 0.01$, ****$p < 0.0001$).

mice at 5 days p.i., due to the downregulation of the DEGs listed (Fig. 4C). STRING network in Fig. 4E is centered around *Il6,* similarly to what was observed at 1 day p.i. (Fig. S1), although at 5 days p.i. most genes are downregulated in infected mice.

At 10 days p.i., 116 genes were differentially expressed between infected and control mice (DE), 49 of them were statistically significant upregulated (red dots in Fig. 5A and B) and 67 of them were statistically significant downregulated (blue dots in Fig. 5A and C). STRING interaction networks including these 116 genes are shown in Fig. S2.

3.3. Immunometabolic pathways over-representation through the course of the early Leishmania infantum infection in the spleen of BALB/c mice

The day-by-day analysis of enriched pathways during the early *L. infantum* infection in the spleen, reveals an evolving pattern of gene expression. To compare this evolution, we used the Top 10 enriched pathways at each timepoint (with upregulated and downregulated genes, separately) (Table S3), and summarized the enrichment in Fig. 6. Moreover, this analysis reveals some genes that are relevant due to their up- or downregulation along the course of the experiment.

The only pathway over-represented by downregulated genes at all timepoints, from day 1 to day 10 p.i., was *Cellular response to organic substance.* Besides, the downregulation escalated along the course of the experiment showing progressively lower FDR values, something that was also evident for some other pathways like *Icosanoid biosynthetic process, Th17 cell differentiation, Leukocyte chemotaxis* and *Cell population proliferation.* (Fig. 6). Genes involved in these pathways were significantly downregulated at 3, 5 and 10 days p.i., particularly *Alox12, Alox5* or *Rxra.* (Table S4, Fig. 7).

Some pathways were predominantly enriched (from downregulated genes) from day 5 p.i. onwards (*HIF-1 signaling pathway, Carboxylic acid biosynthetic process, Adipocytokine signaling pathway* and *apoptotic cell clearance)* (Fig. 6), a finding probably related to the leap in parasite burden observed at 5 and 10 days p.i. The over-representation of these pathways involved statistically significant downregulation of a number of genes at 5- and 10- days p.i., such as *Mtor* and *Ldha* (*HIF-1 signaling pathway); Alox12, Nr1h3, Alox5, Ldha* and *Tpi1 (Carboxylic acid biosynthetic process); Mtor* and *Rxra (Adipocytokine signaling pathway); Tgm2* and *Nr1h3 (Apoptotic cell clearance); Tgm2 (Positive regulation of cell adhesion)* and *Il1rap* (*Regulation of cytokine secretion)* (Table S4, Fig. 7).

In contrast to that deepening pattern observed for downregulated pathways, the enrichment with upregulated genes through the course of the infection revealed lower FDR values, therefore largest over-representation, at 1- and 10-days p.i. (Fig. 6). Four pathways related to activation of immune system responses were over-represented at all timepoints (Fig. 6), with *Il21* emerging as a major marker of this activation due to its significant upregulation at all timepoints (Fig. 8).

Other pathways were over-represented at 1, 3 and 10 days p.i. (Fig. 6), such as *Response to other organism, Regulation of regulatory T cell differentiation, Th1 and Th2 cell differentiation, Regulation of inflammatory response, Positive regulation of isotype switching to IgG isotypes, Regulation of lymphocyte apoptotic process,* and *Apoptotic signaling pathway*. From these pathways, several genes arise as important for the early response in spleen tissue to *L. infantum* infection, like *Il2*, involved in most of those annotations, *Tbx21 (Th1 and Th2 cell differentiation, Response to other organism* and *Positive regulation of isotype switching to IgG isotypes); Ptgs2 (Response to other organism, Regulation of inflammatory response* and *Positive regulation of inflammatory response); Pdcd1,* also upregulated, is involved in *Regulation of lymphocyte apoptotic process* (Fig. 8, Table S4).

4. Discussion

The analysis of transcriptional changes over the course of *Leishmania* infection, using different methodologies, have shown the main mechanisms that describe the complex immune responses in the host. However, those analyses diverge not only in the methodology used (RNA-seq, microarray, qPCR…), but also in the animal model, the *Leishmania* species, or even the tissue or cells analyzed, therefore the results are difficult to compare. In the literature, despite the Syrian golden hamster model mimicking some pathophysiological characteristics observed in human infections, most of the transcriptional analyses during *Leishmania* infection have been developed either in the early or chronic phase of the infection in mice spleen (Ashwin et al., 2019; Forrester et al., 2022; Kong et al., 2017; Ontoria et al., 2018), in splenic $CD4^+$ T cells (Medina-Colorado et al., 2017) or in mouse bone marrow derived macrophages (BMDM) in the initial invasion (from one to 24 h post-infection) (Fortéa et al., 2009; Palacios et al., 2023; Rabhi et al., 2012). The aim of this paper is to analyze, in a time course manner (from 1- through 10-days p.i.), the main transcriptional changes in spleen tissue infected by *L. infantum,* in order to describe the processes and pathways over-represented by downregulated or upregulated genes and related not only to innate immune response but also to metabolism.

As early as 1 day after parasite inoculation, infection is evident in the spleen tissue and splenomegaly is initiating. One of the most notorious clinical features of VL is the splenomegaly (Engwerda and Kaye, 2000). It is known that structural changes in the spleen occur in the chronic phase and those changes are concomitant with the increased organ mass and size (Engwerda and Kaye, 2000). The transcriptional profile at this early timepoint reveals upregulation of dozens of genes involved in activation of inflammatory responses, Th cell differentiation, leukocyte immunity or chemokine signaling. This suggests an extremely swift activation of immune response in spleen tissue, including early signs for cell recruitment, particularly of monocytes due to *Ccl2* upregulation, among other chemokines (Gordon, 2007; Gordon and Taylor, 2005).

At this timepoint, the main transcriptional changes involve pathways associated to immune response. In *Leishmania* sp. infection, the first inflammatory stimuli after the infection activate pathways (such as NF-κB (Castrillo and Tontonoz, 2004)) for Th1 response through TLR and

A

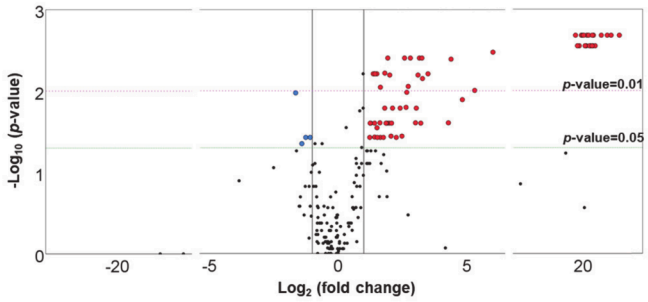

B

UPREGULATED					
GENE	Log_2(FC)	GENE	Log_2(FC)	GENE	Log_2(FC)
STAT2	21.40	CCL7	4.83	TLR4	1.98
TGM2	21.08	CSF2	4.39	PLA2G4A	1.93
IL15	20.93	IL27	4.28	TNFRSF1A	1.89
PDK1	20.70	STAT1	3.49	MYD88	1.86
ITGAL	20.46	IL21	3.28	PDCD1	1.82
IL18R1	20.40	XCL1	3.26	TLR9	1.81
PTP-1B	20.37	IRF7	3.21	LAG3	1.76
JAK2	20.35	CXCL9	3.16	GZMB	1.65
P2X7	20.35	IL4	3.10	TLR3	1.64
UCP2	20.29	IL18BP	3.04	IL27RA	1.63
TPI1	20.25	CCL2	3.01	NFKB1	1.53
LTA4H	20.21	CXCL11	2.81	LTA	1.51
LTB4DH	20.14	IL2	2.73	TNFRSF1B	1.51
MTOR	20.12	IRF1	2.67	CD25	1.43
NFAT5	20.07	IFNG	2.64	TGFBR2	1.42
PGM2	20.01	IL1RN	2.58	CXCL1	1.42
IL1RAP	19.98	IL12RB1	2.48	IL1B	1.42
RXRA	19.93	TBX21	2.41	IL2RB	1.37
JAK1	19.85	CXCL10	2.26	IL21R	1.26
PI3K	19.78	IL1A	2.12	PTGER4	1.25
MRC1	19.70	IL2RG	2.08	CCL19	1.23
IRG1	6.01	IL23R	2.06		
PTGS2	5.30	IL6	2.01		

C

DOWNREGULATED	
GENE	Log_2(FC)
PGES2	-1.64
CXCL13	-1.40
HAVCR2	-1.25
IL1R1	-1.08

D

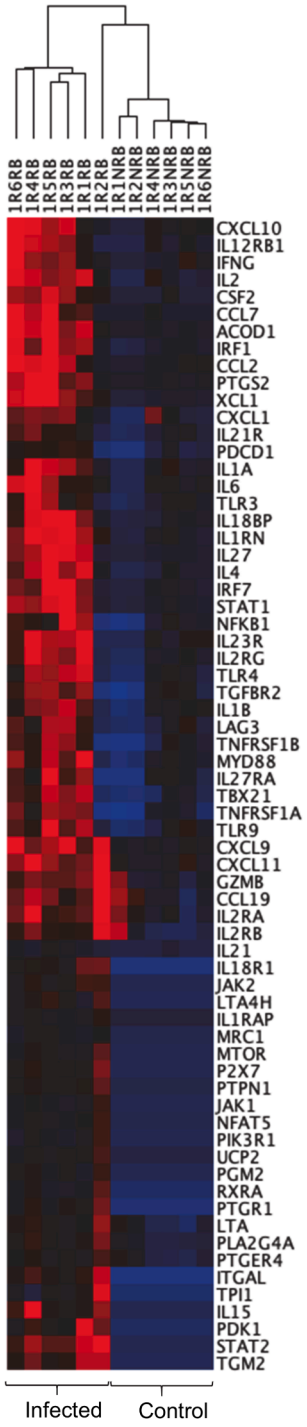

Fig. 2. (A) Volcano plot with the differential expression of 223 analyzed genes in infected ($n = 6$) vs control mice ($n = 6$) at 1 day p.i. Biological threshold is indicated by black vertical lines. Statistical thresholds (p-value=0.05 and p-value= 0.01) are indicated as horizontal lines. Blue and red dots represent differentially expressed genes (DEGs) downregulated and upregulated, respectively. Black dots are genes without significant statistical differences. List of DEGs upregulated (B) and downregulated (C) at 1 day p.i. Log_2FC is indicated for each gene. (D) Unsupervised hierarchal clustering of 1 day p.i. and control mice including genes upregulated with statistical significance differences. Differential expression of selected genes in 1 day p.i.-mice (left side) and control mice (right side) is shown. Each mouse is identified with a respective code. Red gradient indicates the degree of upregulation and blue gradient indicates the degree of downregulation.

TNF signaling. In our data, many genes that participate in *Regulation of T-helper 1 type immune response* pathway were deregulated, most of them upregulated (such as *Il1b* and *Il1rn,* among others) but some of them also downregulated (*Il1r1*). *IL-1R/TLR* superfamily members play an influential role in initiating host innate immune responses and directing adaptive immune responses against invading foreign pathogens (Mogensen, 2009). Parmar et al. (2018) found that *L.* donovani exploited the multitasking function of Tollip (an endocytic adaptor protein) to inhibit TLR/IL-1R signaling–mediated protective immunity during experimental VL. The upregulation of *tollip* has also been observed in the initial phase of *L. amazonensis* infection in BALB/c mouse macrophages (Fortéa et al., 2009). Innate immune receptors belonging to the IL-1R/TLR superfamily might be internalized into lysosomal compartments by Tollip for degradation in L.

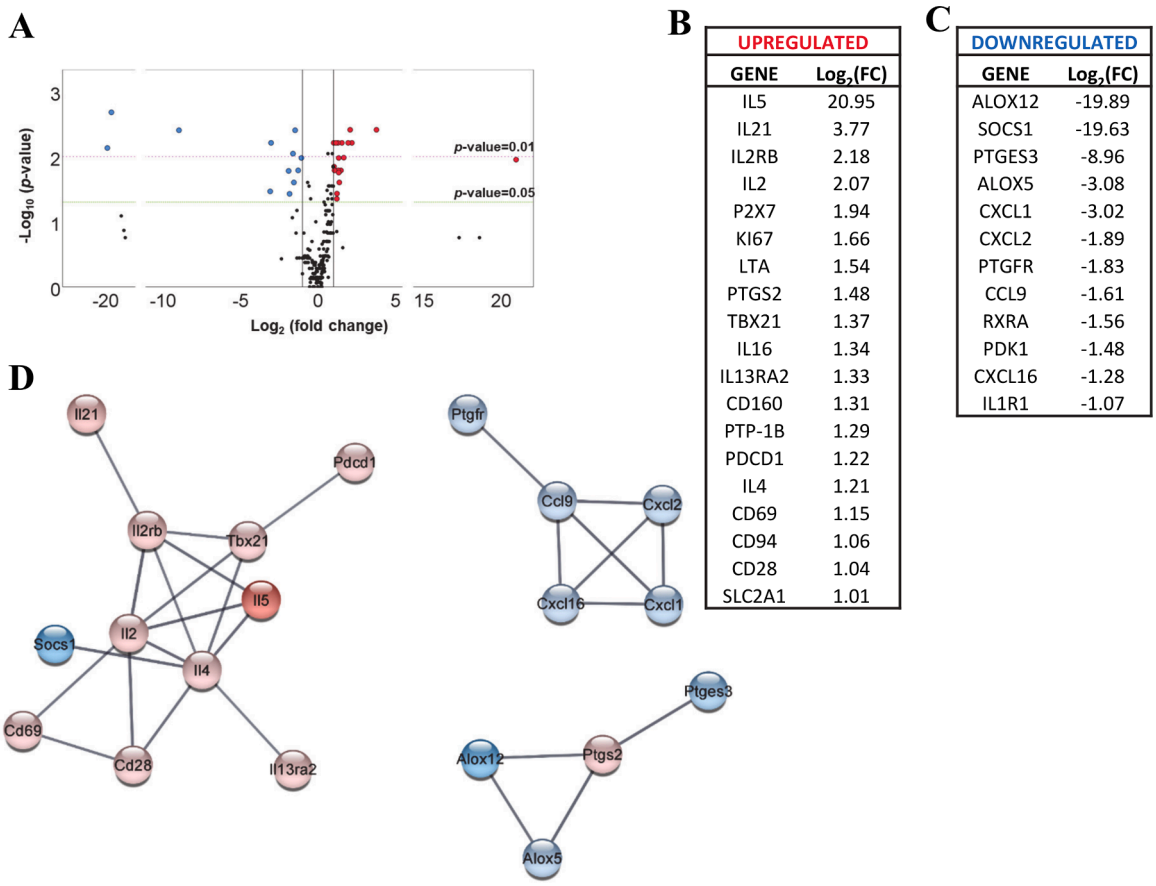

Fig. 3. (A) Volcano plot with the differential expression of 223 analyzed genes in infected (n = 6) vs control mice (n = 6) at 3 days p.i. Biological threshold is indicated by black vertical lines. Statistical thresholds (p-value=0.05 and p-value= 0.01) are indicated as horizontal lines. Blue and red dots represent DEGs downregulated and upregulated, respectively. Black dots are genes without significant statistical differences. List of DEGs upregulated (B) and downregulated (C) at 3 day p.i. Log_2FC is indicated for each gene. (D) STRING Interaction Network. DEGs at 3 days p.i. are represented. Color nodes represent Log_2FC of gene expression. Intensity of color nodes indicates upregulation (more red intensity) and downregulation (more blue intensity). Line thickness indicates the stringdb interaction score.

donovani–infected macrophages. Parmar et al. (2018) observed specific downregulation of IL-1R1 but not TLR2 or TLR4 in infected macrophages, and Tollip played a crucial role in endocytic trafficking of IL-1R1 for its degradation. Those findings are in agreement with the downregulation of *Il1r1* observed at 1 day p.i. Additionally, the IL-1 signaling would be affected in *L. infantum* infection due the upregulation of *Il1rn,* also observed in L. *amazonensis* infection (Fortéa et al., 2009). We hypothesize that the upregulation of *Il1rn* indicates that the association IL1B/IL1RAP is probably inhibited and thus probably NF-κB activation is not being generated through IL-1B signaling. This might be confirmed with further analysis. In our previous study in the liver (Palacios et al., 2021), similar results were obtained with mediators in IL-1 signaling, however we found upregulation of *Il1r1*. Then the inhibition of IL-1 signaling is not clear in the early infection in the liver.

Our results contrast with others that have shown upregulation of many markers involved in metabolic pathways in a very early stage of *L. major* infection of mouse bone marrow-derived macrophages (Rabhi et al., 2012). Rabhi et al. observed many metabolic markers upregulated at 24 h p.i., particularly more than two-fold expression in genes involved in Prostaglandin synthesis (*Pla2g4a, Ltb4dh, Ptger4, Ptges, Ptgs2),* Glycolysis pathway (*Slc2a1, Pfkl, Tpi1, Pdk1),* TCA cycle (*Ldha)* and Cholesterol pathway (*Scl2, Cd36)*. In our data, only *Ltb4dh, Ptger4, Ptgs2* and *Tpi1* showed more than two-fold expression at 1 day p.i., but it is important to consider that our results are from spleen tissue, where transcriptional changes respond to the diverse cellular context in the spleen.

Although no significant changes were observed in the parasite load in spleen between days 1 and 3 days p.i., the gene expression profiles were different. At 3 days p.i. the general activation observed at 1 day p.i. weakens and a similar number of genes were upregulated and downregulated. Remarkably, signals of inhibition of lymphocyte and neutrophil chemotaxis, and icosanoid biosynthesis, coupled to enrichment of cytokine signaling pathways, arise at this time, anticipating the shift that will be evident at later timepoints.

At 5 days p.i., a sharp increase is observed both in parasite burden and spleen weight. The downregulation of genes related to immune response deepens, with 37 statistically significant downregulated genes, particularly *Ccl9, Ccr1, Tgfb2, Cxcr2, Ccr2, Cxcr5,* all related to the overrepresentation of *Leukocyte chemotaxis* pathway. Despite this, there was upregulation of *Ccl7,* a pleiotropic chemokine involved in recruitment of all major leukocyte classes, particularly monocytes and neutrophils (Menten et al., 2001; Navas et al., 2014). CCL7 binds to CCR1 and CCR2, and the genes that encode those markers were downregulated in our data. Taken together, the transcriptional profile at 5 days p.i. suggests disruption of many signals important for leukocyte chemotaxis.

Another signal of transcriptional deregulation that could promote parasite infection is the downregulation of *Lxra*. This transcriptional factor is considered crucial for the development of macrophages in the marginal zone of the spleen (A-Gonzalez et al., 2013; Davies et al., 2013; den Haan and Kraal, 2012; Wculek et al., 2022). The downregulation observed for *Lxra* gene at 5 days p.i. could be related to the downregulation of chemokine receptors in macrophages, and therefore could be an important transcriptional change modulated by the infection to counteract the response generated by MZM and MMM. LXR signaling

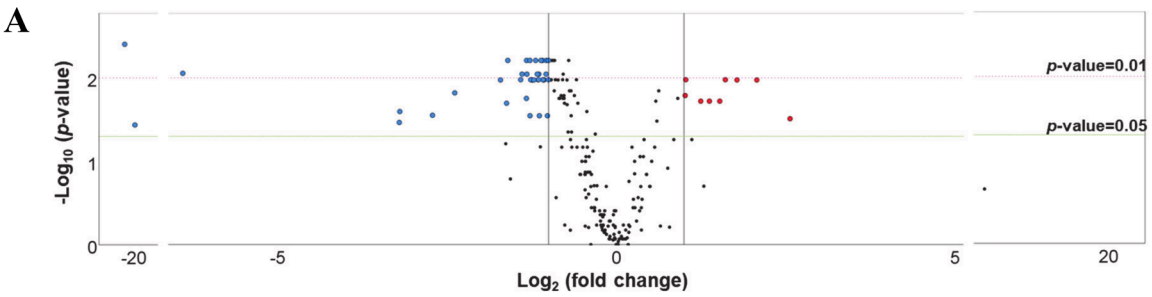

B

UPREGULATED	
GENE	Log_2(FC)
CCL7	2.57
PTGFR	2.07
IL21	1.78
PDCD1LG2	1.61
IL16	1.53
ITGAM	1.38
CD160	1.25
UCP2	1.03
IL13RA2	1.02

C

DOWNREGULATED					
GENE	Log_2(FC)	GENE	Log_2(FC)	GENE	Log_2(FC)
SOCS3	-20.13	PGM2	-1.33	TGFB2	-1.15
IL17F	-19.98	NR1H3	-1.32	CCR2	-1.14
ARG1	-6.40	RXRA	-1.32	IL22RA2	-1.14
ALOX12	-3.20	TPI1	-1.28	LDHA	-1.11
PTGES3	-3.20	ALOX15	-1.27	HAVCR2	-1.09
IL22RA1	-2.71	IL5RA	-1.26	CD86	-1.08
ALOX5	-2.39	IL6	-1.26	ICAM2	-1.07
P2Y2	-1.71	IL23R	-1.24	IFNGR2	-1.07
IL1RAP	-1.62	IL10RB	-1.22	TGM2	-1.04
CCL9	-1.60	CD80	-1.19	CSF2RB	-1.03
MTOR	-1.41	EBI3	-1.17	CCR1	-1.02
MRC1	-1.39	CXCR2	-1.15	ICOSL	-1.00
				CXCR5	-1.00

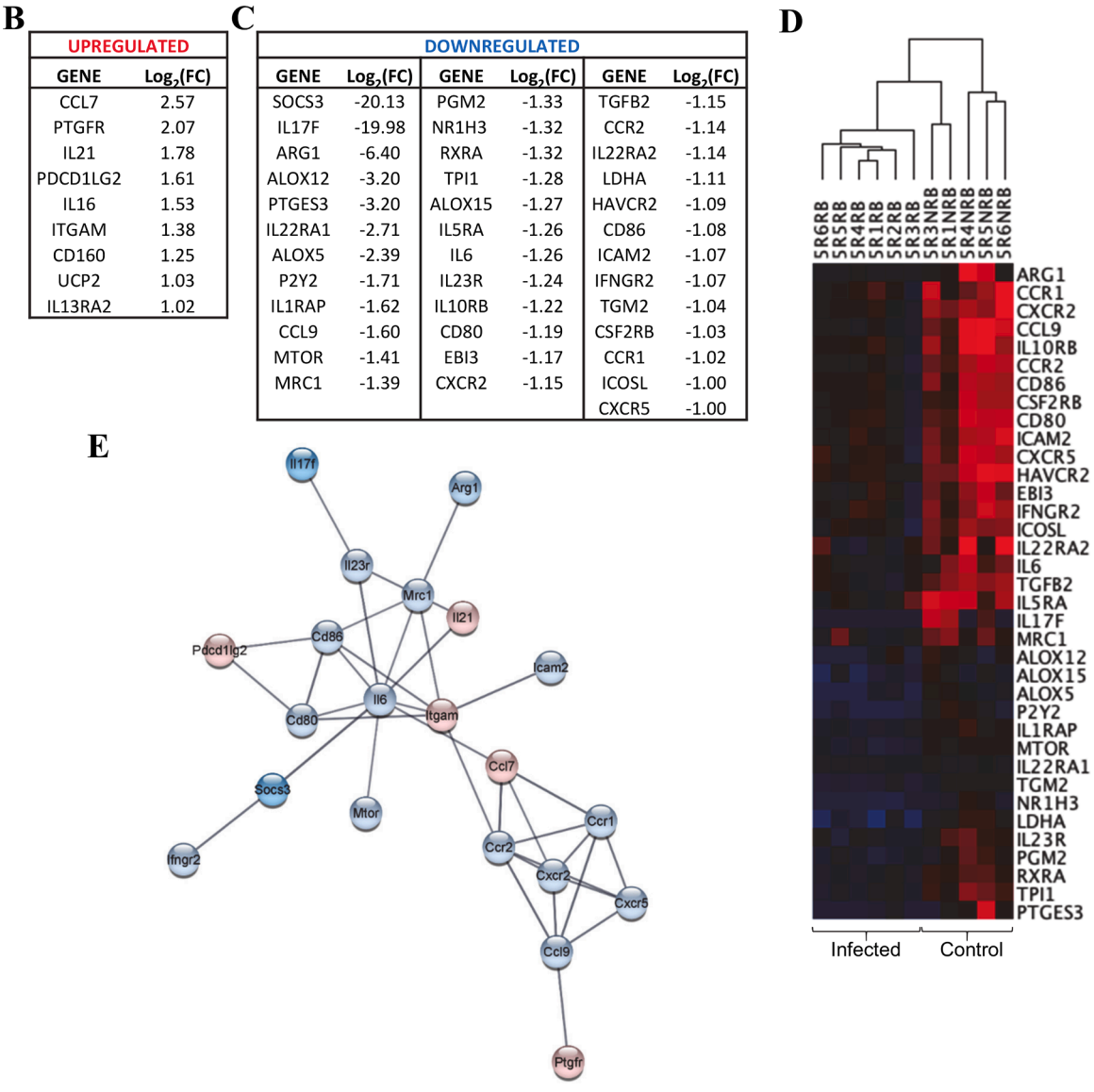

Fig. 4. (A) Volcano plot with the differential expression of 223 analyzed genes in infected (n = 6) vs control mice (n = 5) at 5 days p.i. Biological threshold is indicated by black vertical lines. Statistical thresholds (p-value=0.05 and p-value= 0.01) are indicated as horizontal lines. Blue and red dots represent DEGs downregulated and upregulated, respectively. Black dots are genes without significant statistical differences. List of DEGs upregulated (B) and downregulated (C) at 5 day p.i. Log_2FC is indicated for each gene. (D) Unsupervised hierarchal clustering of 5 days p.i and control mice including genes downregulated with statistical significance differences. Differential expression of selected genes in 5 days p.i.-mice (right side) and control mice (left side) is shown. Each mouse is identified with a respective code. Red gradient indicates the degree of upregulation and blue gradient indicates the degree of downregulation (E) STRING Interaction Network. DEGs at 5 days p.i. are represented. Color nodes represent Log_2FC of gene expression. Intensity of color nodes indicates upregulation (more red intensity) and downregulation (more blue intensity). Line thickness indicates the stringdb interaction score.

also regulates neutrophil homeostasis, and accumulation of apoptotic neutrophils in spleen and liver of LXRαβ–/– mice has been described. (Hong et al., 2012).

Another finding at 5 days p.i. is the over-representation (by downregulated genes) of metabolic pathways, with the downregulation of *Alox12, Alox15, Alox5, Ptges3, Ldha, Nr1h3* and *Tpi1*. The jump in the parasite burden at 5 days p.i. was probably related to the downregulation of those metabolic markers.

A

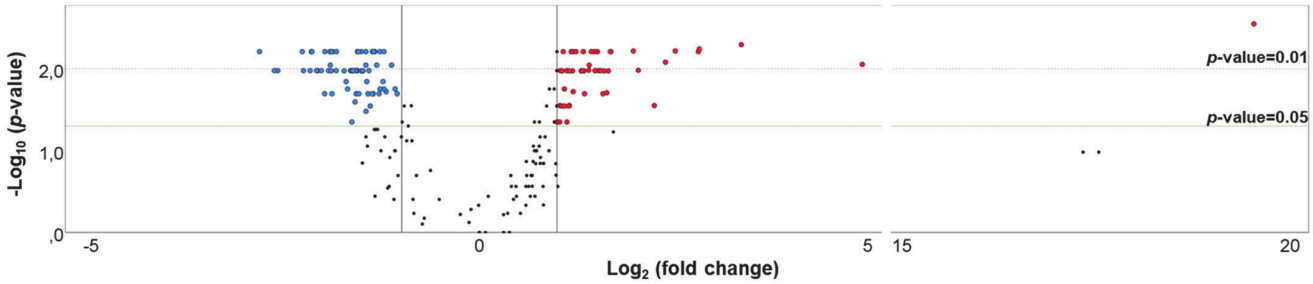

B

UPREGULATED

GENE	Log_2(FC)	GENE	Log_2(FC)	GENE	Log_2(FC)
SOCS1	19.53	XCL1	1.56	HAVCR2	1.20
IL21	4.93	BCL6	1.53	TBX21	1.20
CSF2	3.37	CCR2	1.52	CSF2RB	1.18
IDO1	2.83	CCR5	1.49	IL10RB	1.16
IFNG	2.82	CXCL9	1.49	FOXP3	1.16
IL27	2.52	ICOS	1.48	CD40LG	1.15
CCL7	2.40	CTLA4	1.44	CD274	1.13
PTGS2	2.25	TNF	1.41	IL12RB2	1.13
IL10	2.05	IL12RB1	1.41	CXCR5	1.09
IL2	1.98	CCL4	1.35	IRF1	1.09
ICAM1	1.69	CD40	1.35	ICOSL	1.08
CXCL10	1.69	IL12A	1.34	CD86	1.07
PDCD1	1.66	CXCR3	1.32	IL2RG	1.06
CCL2	1.64	EBI3	1.31	CD83	1.04
STAT1	1.61	IL17RA	1.24	IL23R	1.04
IRG1	1.59	IL18BP	1.21	IFNGR2	1.03
				TGFBR2	1.00

C

DOWNREGULATED

GENE	Log_2(FC)	GENE	Log_2(FC)	GENE	Log_2(FC)	GENE	Log_2(FC)
CD209D	-2.83	CXCR4	-1.90	CCR4	-1.57	ERK2	-1.38
KI67	-2.64	NFAT5	-1.90	AKT3	-1.57	BAX	-1.37
IL22RA1	-2.60	PTP-1B	-1.89	LTB4DH	-1.57	PGM2	-1.36
ALOX12	-2.28	PI3K	-1.84	CD68	-1.56	PFKL	-1.35
PTGDS2	-2.27	BLT1	-1.84	BTLA	-1.55	BCL2	-1.35
PTGS1	-2.18	PDK1	-1.74	PDCD1LG2	-1.52	P38MAPK	-1.32
TGM2	-2.16	LTA4H	-1.72	PTGES	-1.52	TPI1	-1.29
FADD	-2.16	HK1	-1.70	IL1RAP	-1.50	IL10RA	-1.28
PLA2G4A	-2.10	CD4	-1.66	CD169	-1.50	ALOX5	-1.28
BCL2L1	-2.08	IL13RA1	-1.64	IL4RA	-1.46	JAK1	-1.24
UCP2	-2.03	JNK	-1.64	GZMB	-1.46	PGES2	-1.23
CD36	-1.99	ERK1	-1.63	CCL22	-1.46	PFKFB3	-1.23
IL16	-1.99	OX40	-1.63	PTGER4	-1.45	IL15	-1.20
CD94	-1.94	JAK2	-1.60	PTGFR	-1.43	LDHA	-1.13
SLC2A1	-1.92	PTGIS	-1.59	CCL19	-1.42	RXRA	-1.09
MTOR	-1.92	LTA	-1.59	CD69	-1.41	NR1H3	-1.06
CD56	-1.91	CD127	-1.59	GITR	-1.38		

Fig. 5. (A) Volcano plot with the differential expression of 223 analyzed genes in infected ($n = 5$) vs control mice ($n = 6$) at 10 days p.i. Biological threshold is indicated by black vertical lines. Statistical thresholds (p-value=0.05 and p-value= 0.01) are indicated as horizontal lines. Blue and red dots represent DEGs downregulated and upregulated, respectively. Black dots are genes without significant statistical differences. List of DEGs upregulated (B) and downregulated (C) at 10 days p.i. Log_2FC is indicated for each gene.

At 5 days p.i., *Th17 cell differentiation* was also over-represented by downregulated genes. This pathway was found simultaneously over-represented by downregulated and upregulated genes at 3 days p.i. For this reason, the potential inhibition of this pathway is more evident at 5 days p.i., and is sustained at 10 days p.i. This potential inhibition of Th17 pathway would be connected to the downregulation of genes involved in *Carboxylic biosynthetic process,* particularly ALOX5 (5-LO) which has an important role in coordinating the inflammatory immune response involved in the control of VL (Sacramento et al., 2014). 5-LO−/− mice infected with *L. infantum* showed reduced surface co-stimulatory molecule expression and proinflammatory cytokines involved in Th17 differentiation (Sacramento et al., 2014). The statistically significant downregulation of *Alox5*, at 3 and 5 days p.i. would be related to the over-representation (by downregulated genes) of *Th17 cell differentiation.*

At 10 days p.i., both the spleen weight and parasite burden peak, coupled to a strong deregulation of gene expression: up to 116 out 223 genes were up- (49 genes) or downregulated (67 genes) at this timepoint. Many different markers of *T cell migration* pathway were upregulated *(Ccl2, Cxcl10, Cxcr3, Icam1, Cxcl9, Ccr2),* supporting the recruitment of leucocytes, particularly monocytes, at this timepoint in the spleen. Out of these, *Cxcl10* and *Cxcl9* are two markers of M1 response that were identified as important in the early response in previous results in the liver (Palacios et al., 2021).

At this timepoint, we found upregulation of some Treg markers (*Foxp3, Il0* and *Ctla4)* that are associated to $CD4^+CD25^+$ regulatory T cells (Rodrigues et al., 2009; Yamashita et al., 2006). The concomitant expression of *Ifng* and *Il10* suggest that non-FOXP3-expressing Treg subset would also be promoted, as occurred in spleen in the chronic phase (8 weeks p.i.) (Ontoria et al., 2018). *Il10* was also found upregulated overtime in this tissue during *L. donovani* infection (15- 42- days p.i.) (Ashwin et al., 2019). The *Il10*- and *Il21*- mRNA accumulation overtime in the infection by *L. donovani* (Ashwin et al., 2019; Khatonier et al., 2018), together with the sustained *Il21* expression in our study, and *Il10* upregulation at 10 days p.i., define this two genes as important biomarkers of infection in mice spleen.

The upregulation of *Il21* over the timepoints considered in this study is also consistent with the upregulation of this marker in the early chronic phase of the infection in the spleen (at 4 weeks p.i.) in murine model (Ontoria et al., 2018). The upregulation of this gene was also evident in severe human VL (de Melo et al., 2021). IL-21 has been shown to play a role specifically in M2 polarization by decreasing NOS2 expression and increasing STAT3 phosphorylation (Li et al., 2013). The actual potentiality of this molecule as a biomarker of VL remains to be determined, but it is remarkable how this molecule seems to be relevant for parasite progression from the very first moments of VL until the late stages of disease, in different models.

The upregulation of *Il21* together with the upregulation of other inhibitory markers such as *Ctla4, Lag3, Pdcd1* and *Tim3* at 10 days p.i., suggests that T cell exhaustion mechanisms are sustained over the course of the infection. Some of this inhibitory markers have also been described to be induced during *L. amazonensis* infection and its ligands have been used as therapeutic targets (da Fonseca-Martins et al., 2019). In fact, the blockade of PD-1 and PD-L1 induced a strong NK cell response supporting the use of those markers in immunotherapy (Hsu et al., 2018). In addition, an interesting result was observed in dogs

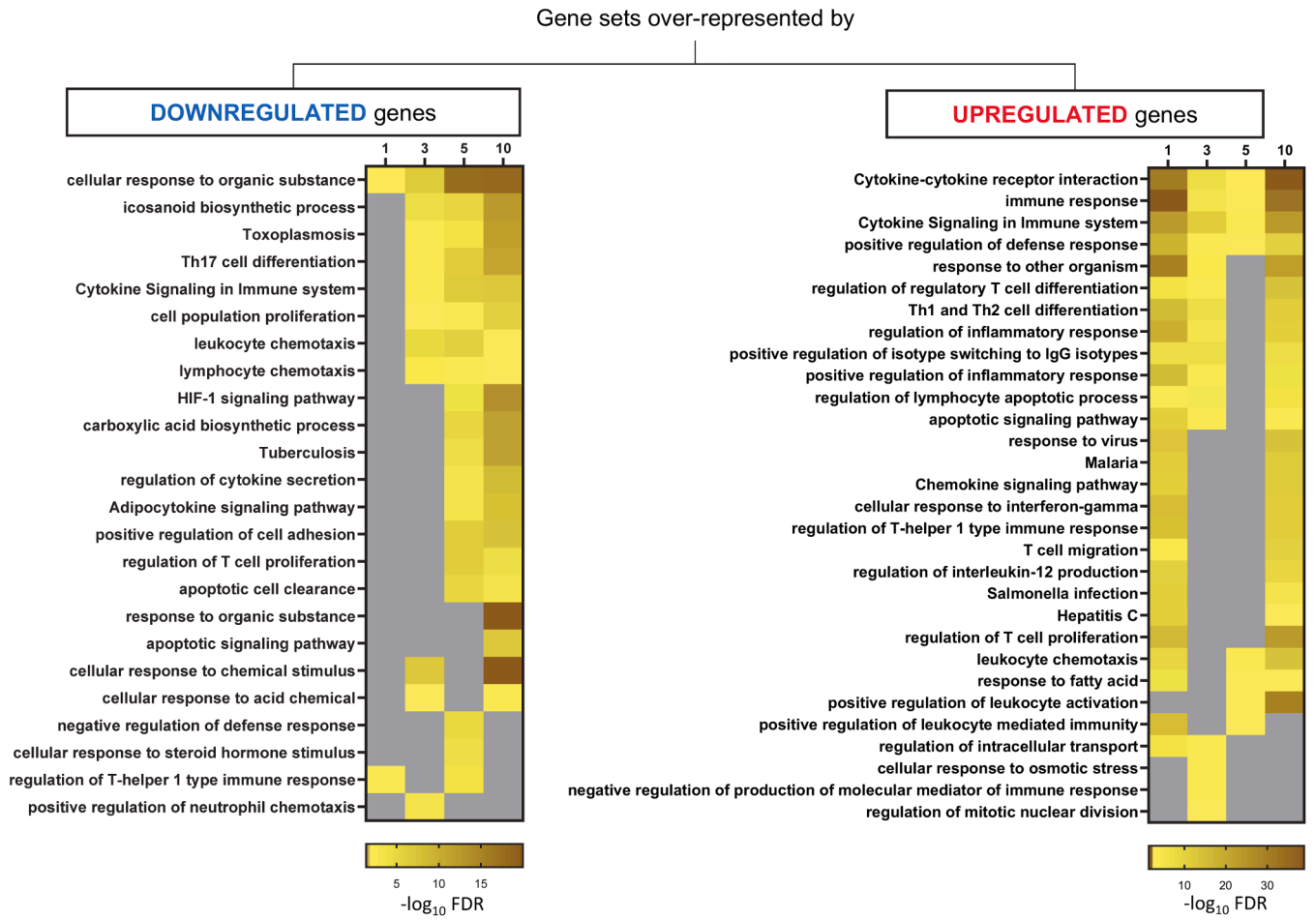

Fig. 6. Heatmaps representing -Log_{10} FDR of gene sets that were over-represented by downregulated or upregulated genes (DEGs), respectively at each timepoint (1-, 3-, 5- and 10- days p.i.). Only gene sets that were enriched after removing redundant terms and in the Top 10 of gene sets with lowest FDR at each timepoint are included. Color intensity of blocks represents significance of enrichment. Gray blocks represent gene sets that were not significantly enriched at a given timepoint according the defined criteria.

naturally infected with *L. infantum*: these inhibitory markers were expressed at lower levels in dogs with greater splenic white pulp disorganization and higher parasite load, possibly explained as a consequence of cell apoptosis (de Souza et al., 2019).

Similarly, the upregulation of *Ifng* and *Il10* in our study is consistent with results obtained in the hamster model during the infection by *L. donovani*. The IFN-γ-induced activation of STAT3 and expression of IL-10, suggested that splenic macrophages in VL are conditioned to respond to macrophage activation signals with a counter-regulatory response that is ineffective and even disease-promoting (Kong et al., 2017).

It is interesting the non-differential expression of *Nos2,* which is a potent Th1 marker. Previous results obtained in liver infection, showed upregulation of this gene almost in all timepoints evaluated (1-, 3- and 10- days p.i.) (Palacios et al., 2021). This would also support that the Treg and T cell exhaustion promote an ineffective response towards the reduction of parasite burden in the spleen.

The upregulation of many M1 markers at 10 days p.i. (Table S5) is consistent with the over-representation of *HIF-1 signaling pathway* by many downregulated genes. HIF-1α is involved in driving the polarization towards M2-like macrophages and rendering intermediate stage monocytes more susceptible to *L. donovani* infection; it also hampers dendritic cell function and Th1 generation during chronic VL (Hammami et al., 2018, 2017).

Our results are the first to demonstrate transcriptional changes that anticipate the early chronic phase in *L. infantum* infection in the spleen of BALB/c mice. These changes play a role in downregulation of many mediators involved in metabolic processes. At 10 days p.i., although the transcriptional profile in our model is characterized by the downregulation of some MAPKs markers such as *Mapk14, Ptgis, Lta, Ptger4, Jak2, Pla2g4a, Tgm2* and *Nr1h,* and anti-inflammatory signals (upregulation of *Il10* and *Il10rb*), the upregulation of proinflammatory cytokines such as *Il2, Ifng, Tnf, Cxcl10, Cxcl9* indicates that at this timepoint, the expression profile constitutes a mixed milieu of proinflammatory and anti-inflammatory signals.

Sustained downregulation of transcriptional factors such as *Rxra* and *Lxra* after day 3 p.i. suggests inhibition of lipid metabolism routes like cholesterol efflux and fatty acid metabolism, despite the over-representation of *Response to fatty acid* annotation (by upregulated genes) at 5 days p.i. Interestingly, these two genes showed also downregulation during the early infection in the liver of BALB/c mice, but returned to basal levels by day 10 p.i. (Palacios et al., 2021). The inhibition of these two markers could explain the upregulation of pro-inflammatory and M1 markers at 10 days p.i. However, the upregulation of some M2 at 10 days p.i., (such as *Il10, Il21* and *Socs1)* and the upregulation of Treg markers and T cell exhaustion markers at this timepoint, suggests a mixed M1/M2 response in infected cells, unable to mount an effective response for the elimination or reduction of the parasite load in the spleen.

Large scale transcriptional analysis has emerged as a valuable tool for detecting changes in complex biological scenarios, although, similarly to all technologies, showing highlights and limitations. For example, RNA-seq methodologies generate vast amounts of data, but the

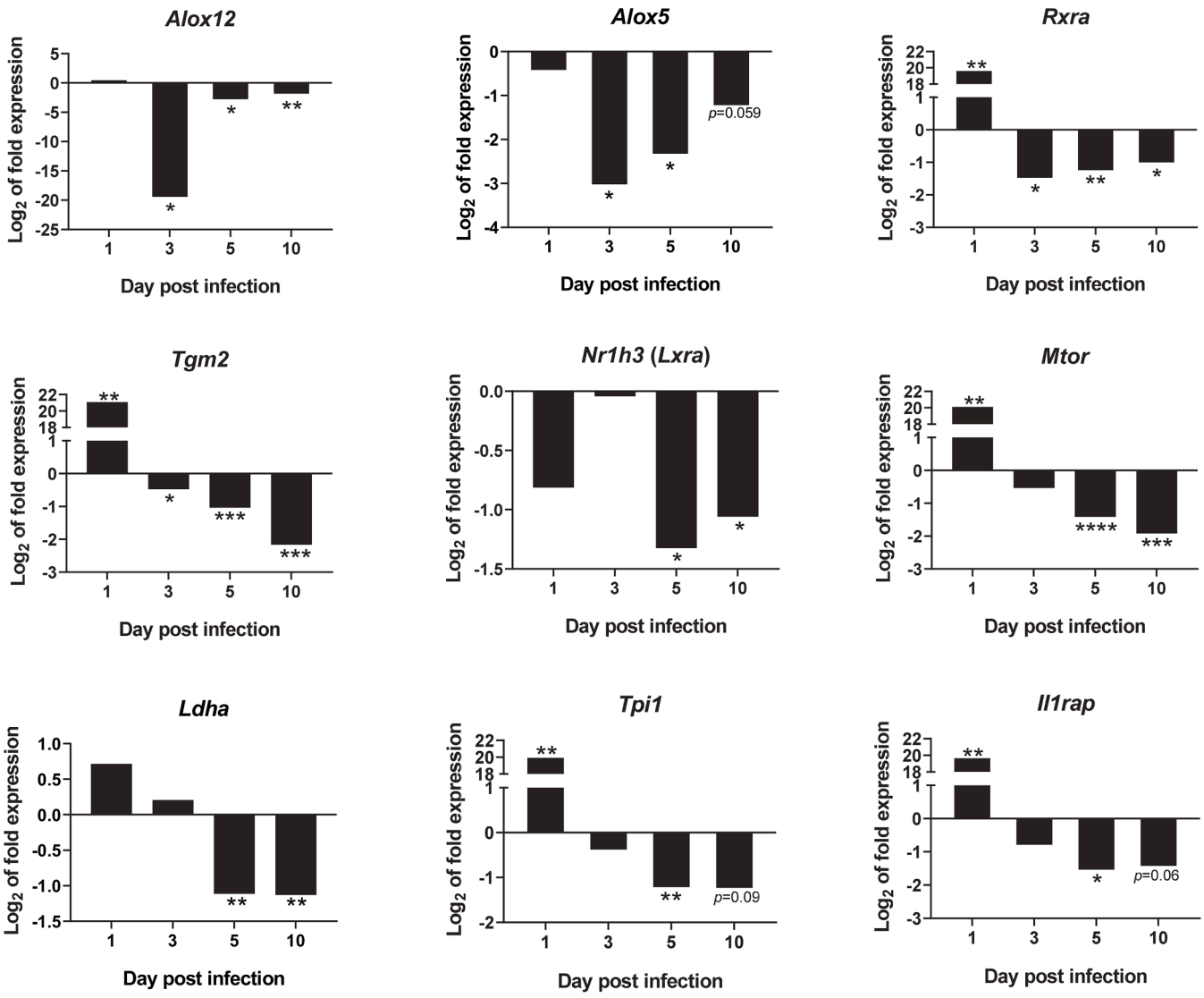

Fig. 7. Common genes in over-represented pathways by downregulated genes at 3-, 5- and 10-days p. i.. mRNA expression at 1-, 3-, 5- and 10-days p.i. expressed as Log_2 of expression fold-change. Statistically significant differences between non- infected (control) and infected animals are indicated (*$p<0.05$; **$p<0.01$; ***$p<0.001$; ****$p<0.0001$).

results are sometimes challenging to relate to the specific topic of interest, and often need confirmation using RT-qPCR (Beattie et al., 2013; Dillon et al., 2015; Fernandes et al., 2016; Ontoria et al., 2018). Conversely, the development of high-throughput RT-qPCR platforms, although provide partial information, enable large-scale gene-expression analysis of extensive gene collections, facilitating the identification of global response patterns in different clinical situations, including human infections (Gómez et al., 2023, 2021). Either way, the results should be complemented with biological analysis to detect expression of the actual markers, not just the genes. Similarly, the identification of a particular pathway as over-represented does not imply its upregulation, since enrichment may be driven either by up- or down-regulation of genes, and this should be taken into account when inferring possible activation or inhibition of routes or pathways.

Finally, the results presented in this study, together with the results previously obtained in the liver (Palacios et al., 2021), allowed to draw the picture of the early *L. infantum* infection in the main target organs in BALB/c mice, in order to identify the main immunological mechanisms involved in the parasite-host interaction.

Supplementary materials

Table S1: List of TaqMan assays used for RT-qPCR analysis using Quant Studio ™ 12 K Flex Real-Time PCR System; Table S2: Functional Enrichment analysis with downregulated or upregulated genes at each timepoint; Table S3: Top 10 annotations from Functional Enrichment analysis with downregulated or upregulated genes at each timepoint.

Funding

We would like to acknowledge the funding provided by Universidad de La Laguna (ULL). GP was supported by "Programa de ayudas a la formación del personal investigador para la realización de tesis doctorales en Canarias de la Consejería de Economía, Industria, Comercio y Conocimiento cofinanciada en un 85% por el Fondo Social Europeo", TESIS2019010018.

Institutional review board statement

Experiments involving animals were conducted in accordance to both European (2010/63/UE) and Spanish legislation (Law 53/2013),

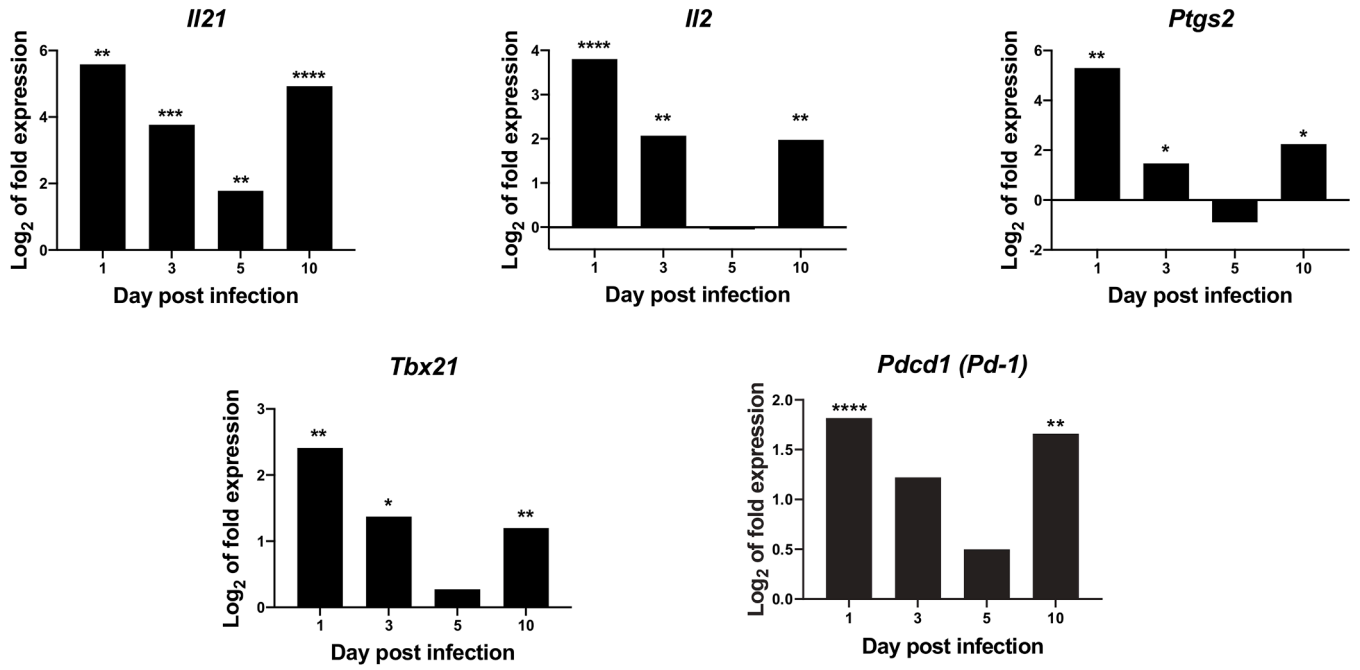

Fig. 8. Selected upregulated genes in over-represented pathways. mRNA expression at 1-, 3-, 5- and 10-days p.i. expressed as Log_2 of expression fold-change. Statistically significant differences between non- infected (control) and infected animals are indicated (*$p<0.05$; **$p<0.01$; ***$p<0.001$; ****$p<0.0001$).

after approval by the Committee for Research Ethics and Animal Welfare (CEIBA) of the University of La Laguna (Permission code: CEIBA2015–0168).

CRediT authorship contribution statement

Génesis Palacios: Conceptualization, Methodology, Software, Validation, Formal analysis, Investigation, Data curation, Writing – original draft, Visualization. **Raquel Diaz-Solano:** Methodology. **Basilio Valladares:** Funding acquisition. **Roberto Dorta-Guerra:** Formal analysis, Writing – review & editing. **Emma Carmelo:** Conceptualization, Methodology, Validation, Investigation, Resources, Writing – original draft, Writing – review & editing, Supervision, Project administration, Funding acquisition.

Declaration of Competing Interest

The authors declare that they have no known competing financial interests or personal relationships that could have appeared to influence the work reported in this paper.

Data availability

Data will be made available on request.

Supplementary materials

Supplementary material associated with this article can be found, in the online version, at doi:10.1016/j.actatropica.2023.107005.

References

A-Gonzalez, N., Guillen, J.A., Gallardo, G., Diaz, M., de la Rosa, J.V., Hernandez, I.H., Casanova-Acebes, M., Lopez, F., Tabraue, C., Beceiro, S., Hong, C., Lara, P.C., Andujar, M., Arai, S., Miyazaki, T., Li, S., Corbi, A.L., Tontonoz, P., Hidalgo, A., Castrillo, A., 2013. The nuclear receptor LXRα controls the functional specialization of splenic macrophages. Nat. Immunol. 14, 831–839. https://doi.org/10.1038/ni.2622.

Abidin, B.M., Hammami, A., Stäger, S., Heinonen, K.M., 2017. Infection-adapted emergency hematopoiesis promotes visceral leishmaniasis. PLOS Pathog 13, e1006422. https://doi.org/10.1371/journal.ppat.1006422.

Ashwin, H., Seifert, K., Forrester, S., Brown, N., MacDonald, S., James, S., Lagos, D., Timmis, J., Mottram, J.C., Croft, S.L., Kaye, P.M., 2019. Tissue and host species-specific transcriptional changes in models of experimental visceral leishmaniasis. Wellcome Open Res. 3, 135. https://doi.org/10.12688/wellcomeopenres.14867.2.

Beattie, L., d'El-Rei Hermida, M., Moore, J.W.J., Maroof, A., Brown, N., Lagos, D., Kaye, P.M., 2013. A transcriptomic network identified in uninfected macrophages responding to inflammation controls intracellular pathogen survival. Cell Host Microbe 14, 357–368. https://doi.org/10.1016/j.chom.2013.08.004.

Buffet, P.A., Sulahian, A., Garin, Y.J., Nassar, N., Derouin, F., 1995. Culture microtitration: a sensitive method for quantifying *Leishmania infantum* in tissues of infected mice. Antimicrob. Agents Chemother. 39, 2167–2168. https://doi.org/10.1128/AAC.39.9.2167.

Castrillo, A., Tontonoz, P., 2004. Nuclear receptors in macrophage biology: at the crossroads of lipid metabolism and inflammation. Annu. Rev. Cell Dev. Biol. 20, 455–480. https://doi.org/10.1146/annurev.cellbio.20.012103.134432.

da Fonseca-Martins, A.M., Ramos, T.D., Pratti, J.E.S., Firmino-Cruz, L., Gomes, D.C.O., Soong, L., Saraiva, E.M., de Matos Guedes, H.L., 2019. Immunotherapy using anti-PD-1 and anti-PD-L1 in Leishmania amazonensis-infected BALB/c mice reduce parasite load. Sci. Rep. 9, 20275. https://doi.org/10.1038/s41598-019-56336-8.

Davies, L.C., Jenkins, S.J., Allen, J.E., Taylor, P.R., 2013. Tissue-resident macrophages. Nat. Immunol. 14, 986–995. https://doi.org/10.1038/ni.2705.

de Melo, C.V.B., Guimarães Torres, F., Hermida, M.D.R., Fontes, J.L.M., Mesquita, B.R., Brito, R., Ramos, P.I.P., Fernandes, G.R., Freitas, L.A.R., Khouri, R., Costa, C.H.N., dos-Santos, W.L.C., 2021. Splenic transcriptional responses in severe visceral leishmaniasis: impaired leukocyte chemotaxis and cell cycle arrest. Front. Immunol. 12 https://doi.org/10.3389/fimmu.2021.716314.

de Souza, T.L., da Silva, A.V.A., Pereira, L., de, O.R., Figueiredo, F.B., Mendes Junior, A. A.V., Menezes, R.C., Mendes-da-Cruz, D.A., Boité, M.C., Cupolillo, E., Porrozzi, R., Morgado, F.N., 2019. Pro-cellular exhaustion markers are associated with splenic microarchitecture disorganization and parasite load in dogs with visceral Leishmaniasis. Sci. Rep. 9 https://doi.org/10.1038/s41598-019-49344-1.

den Haan, J.M., Kraal, G., 2012. Innate immune functions of macrophage subpopulations in the spleen. J. Innate Immun. 4, 437–445. https://doi.org/10.1159/000335216.

Dillon, L.A.L., Suresh, R., Okrah, K., Corrada Bravo, H., Mosser, D.M., El-Sayed, N.M., 2015. Simultaneous transcriptional profiling of Leishmania major and its murine macrophage host cell reveals insights into host-pathogen interactions. BMC Genomics 16, 1108. https://doi.org/10.1186/s12864-015-2237-2.

Engwerda, C.R., Kaye, P.M., 2000. Organ-specific immune responses associated with infectious disease. Immunol. Today 21, 73–78. https://doi.org/10.1016/S0167-5699(99)01549-2.

Fernandes, M.C., Dillon, L.A.L., Belew, A.T., Bravo, H.C., Mosser, D.M., El-Sayed, N.M., 2016. Dual transcriptome profiling of leishmania -infected human macrophages reveals distinct reprogramming signatures. mBio 7, 16. https://doi.org/10.1128/mBio.00027-16.

Forrester, S., Goundry, A., Dias, B.T., Leal-Calvo, T., Moraes, M.O., Kaye, P.M., Mottram, J.C., Lima, A.P.C.A., 2022. Tissue specific dual RNA-Seq defines host–parasite interplay in murine visceral leishmaniasis caused by Leishmania

donovani and *Leishmania infantum*. Microbiol. Spectr. 10, e0067922 https://doi.org/10.1128/spectrum.00679-22.
Fortéa, J.O.y., de La Llave, E., Regnault, B., Coppée, J.Y., Milon, G., Lang, T., Prina, E., 2009. Transcriptional signatures of BALB/c mouse macrophages housing multiplying Leishmania amazonensis amastigotes. BMC Genom. 10, 119. https://doi.org/10.1186/1471-2164-10-119.
Gómez, I., López, M.C., Egui, A., Palacios, G., Carrilero, B., Benítez, C., Simón, M., Segovia, M., Carmelo, E., Thomas, M.C., 2023. Differential expression profile of genes involved in the immune response associated to progression of chronic Chagas disease. PLoS Negl. Trop. Dis. 17, e0011474 https://doi.org/10.1371/journal.pntd.0011474.
Gómez, I., Thomas, M.C., Palacios, G., Egui, A., Carrilero, B., Simón, M., Valladares, B., Segovia, M., Carmelo, E., López, M.C., 2021. Differential expression of immune response genes in asymptomatic chronic Chagas disease patients versus healthy subjects. Front. Cell. Infect. Microbiol. 11 https://doi.org/10.3389/fcimb.2021.722984.
Gorak, P.M.A., Engwerda, C.R., Kaye, P.M., 1998. Dendritic cells, but not macrophages, produce IL-12 immediately followingLeishmania donovani infection. Eur. J. Immunol. 28, 687–695. https://doi.org/10.1002/(SICI)1521-4141(199802)28:02<687::AID-IMMU687>3.0.CO;2-N.
Gordon, S., 2007. Macrophage heterogeneity and tissue lipids. J. Clin. Invest. 117, 1–4. https://doi.org/10.1172/JCI30992.
Gordon, S., Taylor, P.R., 2005. Monocyte and macrophage heterogeneity. Nat. Rev. Immunol. 5, 953–964. https://doi.org/10.1038/nri1733.
Hammami, A., Abidin, B.M., Charpentier, T., Fabié, A., Duguay, A.P., Heinonen, K.M., Stäger, S., 2017. HIF-1α is a key regulator in potentiating suppressor activity and limiting the microbicidal capacity of MDSC-like cells during visceral leishmaniasis. PLOS Pathog. 13, e1006616 https://doi.org/10.1371/journal.ppat.1006616.
Hammami, A., Abidin, B.M., Heinonen, K.M., Stäger, S., 2018. HIF-1α hampers dendritic cell function and Th1 generation during chronic visceral leishmaniasis. Sci. Rep. 8, 3500. https://doi.org/10.1038/s41598-018-21891-z.
Hernandez-Santana, Y.E., Ontoria, E., Gonzalez-García, A.C., Quispe-Ricalde, M.A., Larraga, V., Valladares, B., Carmelo, E., 2016. The challenge of stability in high-throughput gene expression analysis: comprehensive selection and evaluation of reference genes for BALB/c mice spleen samples in the *Leishmania infantum* infection model. PLoS ONE 11, e0163219. https://doi.org/10.1371/journal.pone.0163219.
Hong, C., Kidani, Y., A-Gonzalez, N., Phung, T., Ito, A., Rong, X., Ericson, K., Mikkola, H., Beaven, S.W., Miller, L.S., Shao, W.H., Cohen, P.L., Castrillo, A., Tontonoz, P., Bensinger, S.J., 2012. Coordinate regulation of neutrophil homeostasis by liver X receptors in mice. J. Clin. Invest. 122, 337–347. https://doi.org/10.1172/JCI58393.
Hsu, J., Hodgins, J.J., Marathe, M., Nicolai, C.J., Bourgeois-Daigneault, M.C., Trevino, T. N., Azimi, C.S., Scheer, A.K., Randolph, H.E., Thompson, T.W., Zhang, L., Iannello, A., Mathur, N., Jardine, K.E., Kirn, G.A., Bell, J.C., McBurney, M.W., Raulet, D.H., Ardolino, M., 2018. Contribution of NK cells to immunotherapy mediated by PD-1/PD-L1 blockade. J. Clin. Invest. 128, 4654–4668. https://doi.org/10.1172/JCI99317.
Kaye, P., Scott, P., 2011. Leishmaniasis: complexity at the host–pathogen interface. Nat. Rev. Microbiol. 9, 604–615. https://doi.org/10.1038/nrmicro2608.
Kaye, P.M., Svensson, M., Ato, M., Maroof, A., Polley, R., Stager, S., Zubairi, S., Engwerda, C.R., 2004. The immunopathology of experimental visceral leishmaniasis. Immunol. Rev. 201, 239–253. https://doi.org/10.1111/j.0105-2896.2004.00188.x.
Khatonier, R., Khan, A.M., Sarmah, P., Ahmed, G.U., 2018. Role of IL-21 in host pathogenesis in experimental visceral leishmaniasis. J. Parasit. Dis. 42, 500–504. https://doi.org/10.1007/s12639-018-1025-8.
Kong, F., Saldarriaga, O.A., Spratt, H., Osorio, E.Y., Travi, B.L., Luxon, B.A., Melby, P.C., 2017. Transcriptional profiling in experimental visceral Leishmaniasis reveals a broad splenic inflammatory environment that conditions macrophages toward a disease-promoting phenotype. PLOS Pathog. 13, e1006165 https://doi.org/10.1371/journal.ppat.1006165.
Lewis, S.M., Williams, A., Eisenbarth, S.C., 2019. Structure and function of the immune system in the spleen. Sci. Immunol. 4, eaau6085. https://doi.org/10.1126/sciimmunol.aau6085.
Li, S., Wang, W., Fu, S., Wang, J., Liu, H., Xie, S., Liu, B., Li, Y., Lv, Q., Li, Z., Xue, W., Huang, B., Chen, W., Liu, J., 2013. IL-21 modulates release of proinflammatory cytokines in LPS-stimulated macrophages through distinct signaling pathways. Mediat. Inflamm. 2013, 1–12. https://doi.org/10.1155/2013/548073.
Loria-Cervera, E.N., Andrade-Narvaez, F.J., 2014. Animal models for the study of leishmaniasis immunology. Rev. Inst. Med. Trop. Sao Paulo 56, 1–11. https://doi.org/10.1590/S0036-46652014000100001.
Medina-Colorado, A.A., Osorio, E.Y., Saldarriaga, O.A., Travi, B.L., Kong, F., Spratt, H., Soong, L., Melby, P.C., 2017. Splenic CD4+ T cells in progressive visceral Leishmaniasis show a mixed effector-regulatory phenotype and impair macrophage effector function through inhibitory receptor expression. PLoS ONE 12, e0169496. https://doi.org/10.1371/journal.pone.0169496.
Melby, P.C., Yang, Y.Z., Cheng, J., Zhao, W., 1998. Regional differences in the cellular immune response to experimental cutaneous or visceral infection with Leishmania donovani. Infect. Immun. 66 https://doi.org/10.1128/iai.66.1.18-27.1998.
Melo, C.V.B., Hermida, M.D.R., Mesquita, B.R., Fontes, J.L.M., Koning, J.J., Solcà, M.S., Benevides, B.B., Mota, G.B.S., Freitas, L.A.R., Mebius, R.E., Dos-Santos, W.L.C., 2020. Phenotypical characterization of spleen remodeling in murine experimental visceral Leishmaniasis. Front. Immunol. 11, 653. https://doi.org/10.3389/fimmu.2020.00653.
Menten, P., Wuyts, A., Van Damme, J., 2001. Monocyte chemotactic protein-3. Eur. Cytokine Netw. 12, 554–560.
Mogensen, T.H., 2009. Pathogen recognition and inflammatory signaling in innate immune defenses. Clin. Microbiol. Rev. 22, 240–273. https://doi.org/10.1128/CMR.00046-08.
Morris, J.H., Apeltsin, L., Newman, A.M., Baumbach, J., Wittkop, T., Su, G., Bader, G.D., Ferrin, T.E., 2011. clusterMaker: a multi-algorithm clustering plugin for cytoscape. BMC Bioinform. 12, 436. https://doi.org/10.1186/1471-2105-12-436.
Navas, A., Vargas, D.A., Freudzon, M., McMahon-Pratt, D., Saravia, N.G., Gómez, M.A., 2014. Chronicity of dermal Leishmaniasis caused by Leishmania panamensis is associated with parasite-mediated induction of chemokine gene expression. Infect. Immun. 82, 2872–2880. https://doi.org/10.1128/IAI.01133-13.
Negron, E., Sanchez, M.A., Diaz, N.L., Convit, J., Tapia, F.J., Zerpa, O., 2004. Organ-specific immunity in canine visceral leishmaniasis: analysis of symptomatic and asymptomatic dogs naturally infected with Leishmania chagasi. Am. J. Trop. Med. Hyg. 70, 618–624. https://doi.org/10.4269/ajtmh.2004.70.618.
Oliveira, D.M., Costa, M.A.F., Chavez-Fumagalli, M.A., Valadares, D.G., Duarte, M.C., Costa, L.E., Martins, V.T., Gomes, R.F., Melo, M.N., Soto, M., Tavares, C.A.P., Coelho, E.A.F., 2012. Evaluation of parasitological and immunological parameters of Leishmania chagasi infection in BALB/c mice using different doses and routes of inoculation of parasites. Parasitol. Res. 110 https://doi.org/10.1007/s00436-011-2628-5.
Ontoria, E., Hernández-Santana, Y.E., González-García, A.C., López, M.C., Valladares, B., Carmelo, E., 2018. Transcriptional profiling of immune-related genes in *Leishmania infantum*-infected mice: identification of potential biomarkers of infection and progression of disease. Front. Cell. Infect. Microbiol. 8, 197. https://doi.org/10.3389/fcimb.2018.00197.
Osorio, E.Y., Medina-Colorado, A.A., Travi, B.L., Melby, P.C., 2020. *In-situ* proliferation contributes to the accumulation of myeloid cells in the spleen during progressive experimental visceral leishmaniasis. PLoS ONE 15, e0242337. https://doi.org/10.1371/journal.pone.0242337.
Palacios, G., Diaz-Solano, R., Valladares, B., Dorta-Guerra, R., Carmelo, E., 2021. Early transcriptional liver signatures in experimental visceral leishmaniasis. Int. J. Mol. Sci. 22, 7161. https://doi.org/10.3390/ijms22137161.
Palacios, G., Vega-García, E., Valladares, B., Pérez, J.A., Dorta-Guerra, R., Carmelo, E., 2023. Gene expression profiling of classically activated macrophages in leishmania infantum infection: response to metabolic pre-stimulus with itaconic acid. Trop. Med. Infect. Dis. 8, 264. https://doi.org/10.3390/tropicalmed8050264.
Parmar, N., Chandrakar, P., Vishwakarma, P., Singh, K., Mitra, K., Kar, S., 2018. Leishmania donovani exploits tollip, a multitasking protein, to impair TLR/IL-1R signaling for its survival in the host. J. Immunol. 201, 957–970. https://doi.org/10.4049/jimmunol.1800062.
Poulaki, A., Piperaki, E.T., Voulgarelis, M., 2021. Effects of visceralising leishmania on the spleen, liver, and bone marrow: a pathophysiological perspective. Microorganisms 9, 759. https://doi.org/10.3390/microorganisms9040759.
Rabhi, I., Rabhi, S., Ben-Othman, R., Rasche, A., Consortium, S., Daskalaki, A., Trentin, B., Piquemal, D., Regnault, B., Descoteaux, A., Guizani-Tabbane, L., 2012. Transcriptomic signature of leishmania infected mice macrophages: a metabolic point of view. PLoS Negl. Trop. Dis. 6, e1763. https://doi.org/10.1371/journal.pntd.0001763.
Rodrigues, O.R., Marques, C., Soares-Clemente, M., Ferronha, M.H., Santos-Gomes, G.M., 2009. Identification of regulatory T cells during experimental *Leishmania infantum* infection. Immunobiology 214, 101–111. https://doi.org/10.1016/j.imbio.2008.07.001.
Rodrigues, V., Cordeiro-da-Silva, A., Laforge, M., Silvestre, R., Estaquier, J., 2016. Regulation of immunity during visceral Leishmania infection. Parasit. Vectors 9, 118. https://doi.org/10.1186/s13071-016-1412-x.
Rolão, N., Melo, C., Campino, L., 2004. Influence of the inoculation route in BALB/c mice infected by *Leishmania infantum*. Acta Trop. 90 https://doi.org/10.1016/j.actatropica.2003.09.010.
Sacramento, L.A., Cunha, F.Q., de Almeida, R.P., da Silva, J.S., Carregaro, V., 2014. Protective Role of 5-Lipoxigenase during *Leishmania infantum* infection is associated with Th17 subset. Biomed Res. Int. 2014, 1–12. https://doi.org/10.1155/2014/264270.
Saini, S., Rai, A.K., 2020. Hamster, a close model for visceral leishmaniasis: opportunities and challenges. Parasite Immunol 42, e12768. https://doi.org/10.1111/pim.12768.
Shannon, P., 2003. Cytoscape: a software environment for integrated models of biomolecular interaction networks. Genome Res. 13, 2498–2504. https://doi.org/10.1101/gr.1239303.
Singh, R.K., Pandey, H.P., Sundar, S., 2006. Visceral leishmaniasis (kala-azar): challenges ahead. Indian J. Med. Res.
Szklarczyk, D., Morris, J.H., Cook, H., Kuhn, M., Wyder, S., Simonovic, M., Santos, A., Doncheva, N.T., Roth, A., Bork, P., Jensen, L.J., von Mering, C., 2017. The STRING database in 2017: quality-controlled protein–protein association networks, made broadly accessible. Nucleic Acids Res. 45, D362–D368. https://doi.org/10.1093/nar/gkw937.
Tibúrcio, R., Nunes, S., Nunes, I., Rosa Ampuero, M., Silva, I.B., Lima, R., Machado Tavares, N., Brodskyn, C., 2019. Molecular aspects of dendritic cell activation in leishmaniasis: an immunobiological view. Front. Immunol. 10, 227. https://doi.org/10.3389/fimmu.2019.00227.
Titus, R.G., Ribeiro, J.M.C., 1988. Salivary gland lysates from the sand fly lutzomyia longipalpis enhance leishmania infectivity. Science 239. https://doi.org/10.1126/science.3344436.
Wculek, S.K., Dunphy, G., Heras-Murillo, I., Mastrangelo, A., Sancho, D., 2022. Metabolism of tissue macrophages in homeostasis and pathology. Cell. Mol. Immunol. 19, 384–408. https://doi.org/10.1038/s41423-021-00791-9.
Yamashita, K., Öllinger, R., McDaid, J., Sakahama, H., Wang, H., Tyagi, S., Csizmadia, E., Smith, N.R., Soares, M.P., Bach, F.H., 2006. Heme oxygenase-1 is essential for and

promotes tolerance to transplanted organs. FASEB J 20, 776–778. https://doi.org/10.1096/fj.05-4791fje.